

# Scientific session of the Division of General Physics and Astronomy of the Russian Academy of Sciences (25 October 1998)

A scientific session of the Division of General Physics and Astronomy of the Russian Academy of Sciences (RAS) was held at the P L Kapitza Institute for Physical Problems, RAS on 25 October 1998. Two papers were presented at the session:

(1) **Elesin V F** (Moscow Engineering Physical Institute, Moscow), **Kopaev Yu V** (P N Lebedev Physics Institute, RAS, Moscow) “Unipolar semiconductor lasers”;

(2) **Snigirev O V** (M V Lomonosov Moscow State University, Physics Department) “Supersensitive SQUID magnetometry”.

An abridged version of the second paper is given below.

PACS numbers: 07.55.+x, 07.60.Ly, 74.70.–b

## Supersensitive SQUID magnetometry

O V Snigirev

### 1. Introduction

Magnetometers built around superconducting quantum interference devices, known as SQUIDs, are presently the most popular instruments among the great variety of non-linear superconducting electronic appliances based on the Josephson effect (see, for instance, Ref. [1]).

A quantum interferometer manufactured using contemporary thin-film techniques is a planar superconducting closed circuit with a characteristic inner loop dimension of about 50 μm [2], so the interferometer inductance is about 10<sup>-10</sup> H, which is essential for optimization of parameters of the magnetometer as a whole [3]. It is precisely small dimensions of the interferometer in combination with the rather high direct sensitivity to an external magnetic field (the noise-equivalent field is of the order of 1 pT Hz<sup>-1/2</sup>) without using input magnetic flux transformers that led the researchers to the idea of visualizing magnetic field patterns with a SQUID in the early 1990s.

Although the schematic diagram of the SQUID microscope (Fig. 1), which was designed to implement the idea of high-resolution, high-sensitivity magnetic imaging, seemed fairly simple, we had to solve several complicated problems to put it into practice. Firstly, given the high SQUID sensitivity to magnetic field, we had to build a scanning gear made from magnetically pure materials with a scan range in the X-Y plane of the order of 1 × 1 cm<sup>2</sup> and scanned positions reproducible within 10 μm at a temperature of 4.2 K or 77 K.

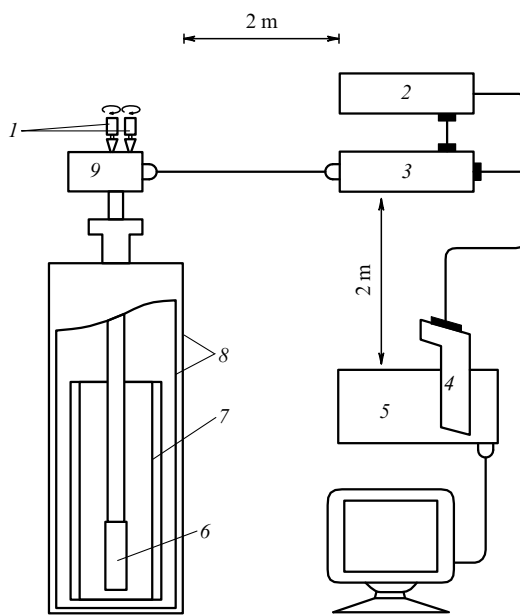


**Figure 1.** Functional diagram of the SQUID magnetometer: 1 — stepping motors; 2 — lock-in amplifier; 3 — electronic unit controlling operation of the system components; 4 — analogue-to-digital converter; 5 — personal computer; 6 — cryogenic scanning X-Y-Z manipulator and quantum interferometer of the microscope; 7 — cryostat; 8 — magnetic shields; 9 — SQUID electronics.

Since the SQUID-microscope space resolution is determined by the larger of the two magnitudes, namely, the interferometer linear dimension and its separation ΔZ from the upper plane of the tested object, the scanning mechanism should be capable of moving the device at ΔZ ranging between 10 and 100 μm.

Secondly, we had a natural desire to operate the facility at a magnetic biasing of up to a highest value of 100 A m<sup>-1</sup>, which would allow comparison of our results with data obtained by different techniques, specifically, magneto-optical [4] or Hall measurements [5]. This led us to make the dimensions of Josephson junctions in the interferometer as small as possible, especially when high-temperature superconductors (HTSC) were used.

Thirdly, the presence of a computer, stepping motors and branched electric circuits with typical lengths of 1–2 m required a system of carefully designed circuits that would filter out electromagnetic interference from signals fed to the interferometer with a view to operating it at the highest possible sensitivity.

In spite of all these difficulties, the first prototypes were built in 1991–1993 [6, 7] and tested on simplest objects, such as patterns of meandering current leads. This paper reports

on the current state of technical design in this field of research and applications of scanning SQUID microscopes (SSM) to physical experiments.

## 2. Scanning mechanism and space resolution

Since most of the potential objects of research by means of SQUID microscopy have dimensions of several millimetres, and the SSM probe (quantum interferometer) should be driven away from the tested sample through a comparable distance in order to define a reference point on the vertical axis, we designed a wedge-and-spring translation stage (Fig. 2). The stage supporting the tested sample is driven by stepping motors. Rotational motion of their shafts is translated into the motion of the ‘X’ and ‘Y’ stages via micrometer screws and springed rods. A similar scheme is used in the gear driving the SQUID with respect to the sample. Since the motors make one revolution per 400 steps and the pitch of the thread in the commercial micrometer screws is 500  $\mu\text{m}$ , the minimal translation step is 1.2  $\mu\text{m}$  for the Y-stage and 0.6  $\mu\text{m}$  for the X-stage, since the X-stage is driven by a wedge set against another wedge so that the translation rate ratio is 2:1. Given a mechanical backlash of about 10  $\mu\text{m}$ , the linear dimensions of the SQUID probe, and the requirements for a minimal scanning time, the optimal scanning step width is 4.8  $\mu\text{m}$ .

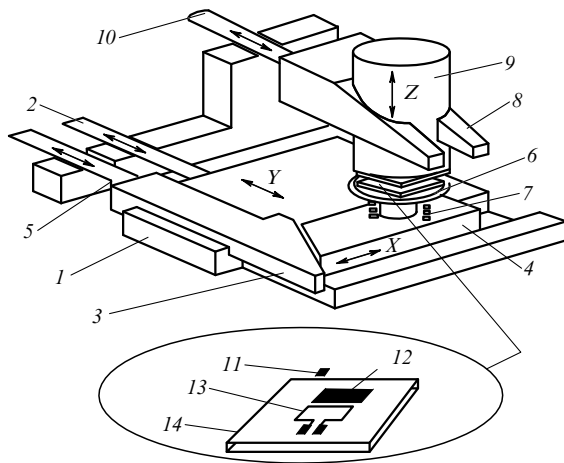


**Figure 2.** Schematic diagram of the cryogenic section of the scanning SQUID microscope: 1 — Y-stage; 2 — lever of Y-stage; 3 — wedge driving X-stage; 4 — X-stage; 5 — lever of X-stage; 6 — sample holder; 7 — springs of sample holder; 8 — tapered fork driving Z-stage; 9 — SQUID holder; 10 — lever of Z-stage supporting the SQUID. The inset shows an expanded view of the SQUID and sample: 11 — SQUID; 12 — sample; 13 — calibrating current loop; 14 — substrate.

In order to minimize the separation  $\Delta Z$  between the SQUID and the tested sample, a contact scanning mode is used in the device: the substrate supporting the SQUID is set on the ‘Z’ stage so that its plane is tilted with respect to the sample plane by a small angle  $\alpha$  (within  $5^\circ$ ). As the SQUID is driven towards the sample set on the springed stage with a calibration loop, the increase in the SQUID output stops when the SQUID substrate touches the sample substrate. In this case  $\Delta Z \approx l_1 \alpha$ , where  $l_1$  is the distance between the substrate edge and the SQUID.

In constructing a modified version of the SSM, we took account of the scanning mechanism flaws detected in operating the prototype and made necessary changes in its design. The minimal scanning step was trimmed to 2  $\mu\text{m}$  without reducing the viewing field, and the ‘ZOOM’ mode with a translation step of 0.2  $\mu\text{m}$  over a  $0.6 \times 0.6$  mm scan range about any point of the tested area was introduced.

## 3. SSM probes

The SSM configuration allows one to use SQUID probes based on either low-temperature or high-temperature superconductors. A SQUID built around Josephson junctions Nb/AIO<sub>x</sub>/Nb that were fabricated using the seven-layer technique is described in detail elsewhere [8]. A general view

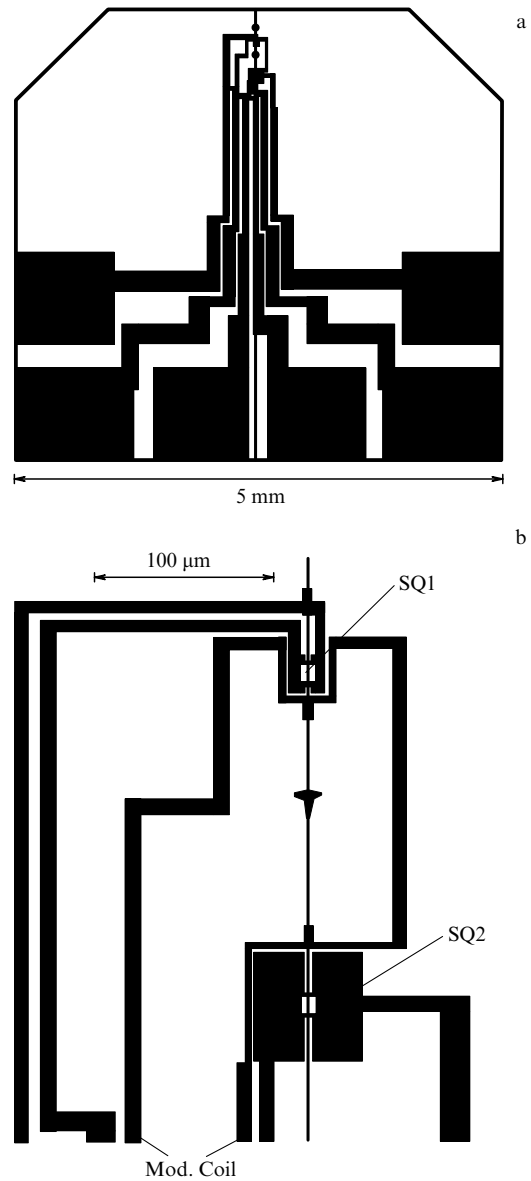


**Figure 3.** Sensor of the SQUID microscope built around HTSC dc SQUIDs: (a) general view of the bicrystalline substrate and the thin-film pattern with contact pads on its surface; (b) expanded diagram of the operating section with two quantum interferometers SQ1 and SQ2 and a common feedback bus (Mod. Coil).

of an SSM probe based on intergranular junctions in a  $\text{YBa}_2\text{Cu}_3\text{O}_{7-x}$  film on a bicrystalline substrate is shown in Fig. 3a, and an expanded view of its operating section including two interferometers, current leads, and a common feedback bus of the SQUID electronics, is shown in Fig. 3b.

Owing to the effect of magnetic flux focusing by the current leads of the single-layer HTSC Josephson junctions [9], the effective area of a 'bridge' junction of width  $W$  is  $W^2/1.84$ , instead of the product of  $W$  times the sum of the London penetration depths  $\lambda_L$  in the current leads. Therefore, a stricter limitation is imposed on the sample magnetization field applied normally to the interferometer plane. If the bridges of widths  $5\ \mu\text{m}$  are fabricated by optical photolithography, the first minimum of the critical current versus magnetic field, where the interferometer output turns to zero, occurs at a field of about  $100\ \text{A m}^{-1}$ . This means that junctions of submicron dimensions manufactured using electronic lithography are required for experiments in magnetic fields of the order of  $1000\ \text{A m}^{-1}$ .

Under a bias field parallel to the interferometer plane, the effective area of an HTSC junction is of order  $2\lambda_L^2$ , and the devices operate normally under magnetic fields of up to  $50\,000\ \text{A m}^{-1}$ . These parameters also apply to niobium probes, which are more susceptible to parallel magnetic fields.

#### 4. Comparison with other devices

Among the devices imaging magnetic field patterns, the scanning SQUID microscope occupies a specific niche. On a diagram that plots the coordinate resolution  $\delta x$  horizontally and the magnetic field resolution  $\delta B$  vertically, the SSM domain is in the lower right-hand corner [10]. It is remarkable that the two main parameters are related by the formula  $\delta B \times (\delta x)^2 = S_{\phi_n}$ , where  $S_{\phi_n}$  is the spectral density of the noise-equivalent magnetic flux of the interferometer.

The devices located most closely to the SSM on this diagram are magneto-optical film imagers [4] and Hall probes based on the two-dimensional electron gas [5]. Even though the space resolution of the latter devices is one order of magnitude smaller, the SSM field resolution within a fixed bandwidth is about three orders of magnitude better. Moreover, SSM is the only device capable of operating at a magnetic biasing below  $50\ \text{A m}^{-1}$ , and the range of this parameter does not have a lower limit.

An important point is that, after the appropriate calibration, SSM allows one to measure accurately the total magnetic moment  $M$  of a sample and its bulk magnetic susceptibility. In this case, the typical magnetic moment resolution is usually smaller than  $10^{-15}\ \text{A m}^2\ \text{Hz}^{-1/2}$ , which corresponds to a sensitivity two or three orders of magnitude higher than that of the previously known instruments built around SQUIDs and measuring magnetic susceptibility.

Given the extraordinarily high SSM sensitivity and its fairly good space resolution, this device shows much promise for physical experiments with extremely small amounts of materials under weak magnetic fields at sample temperatures of 4.2 and 77 K.

#### 5. Conclusions

Thin-film technologies of superconducting materials and techniques for fabrication of Josephson junctions from both low-temperature and high-temperature superconductors, based on intense physical research, have allowed us to build

a unique new device — a scanning SQUID microscope.

Using this device and, accordingly, the techniques of scanning magnetic SQUID microscopy, one can visualize spatial distributions of one magnetic field component in ultrathin films of magnetic materials and in other planar objects, and measure the local magnetization in them in the range of low magnetic fields with a high accuracy unattainable with the help of alternative devices. Presently, the development of an SSM version operating at variable temperatures up to the room temperature is under way.

The work was supported by the Russian Foundation for Basic Research, projects Nos 96-02-19250 and 96-02-18127a, grants from INTAS (No. 93-2777-ext) and BMBF (No. 13N6898), and the 'Superconductivity' subprogramme of the Russian ANFSK state-sponsored R&D programme.

It is a pleasure to express my gratitude to S A Gudoshnikov, K E Andreev, A M Tishin, M Muck, J Dechert, C Heiden, J Bohr, A S Kalabukhov, S A Chupakhin, S I Krasnosvobodtsev, L V Matveets, A V Povolotskiĭ, I G Prokhorova, S N Polyakov, N N Ukhanskiĭ, I I Vengrus, and D E Kirichenko for help at different stages of this work.

#### References

1. Clarke J *Sci. Am.* (8) 36 (Aug. 1994)
2. Ketchen M B *IEEE Trans. Magn.* **MAG-27** 2916 (1991)
3. Danilov V V, Likharev K K, Snigirev O V, in "SQUID '80" (Eds H G Hahlbohm, H Lubbig) (Berlin, New York: Walter de Gruyter, 1980) p. 473
4. Indenbom M V et al. *Physica C* **222** 203 (1994)
5. Oral A, Bending S J, Henini M J. *Vac. Sci. Technol. B* **14** 1202 (1996)
6. Matnai A et al. *IEEE Trans. Appl. Supercond.* **3** 2609 (1993)
7. Gudoshnikov S A et al. *Cryogenics* (UK) **34** (Suppl. issue) 883 (1994)
8. Kirichenko D E et al. *Zh. Tekh. Fiz.* (1999) (in press)
9. Rosenthal P A et al. *Appl. Phys. Lett.* **59** 3482 (1991)
10. Vu L N, Van Harlingen D J *IEEE Trans. Appl. Supercond.* **3** 1918 (1993)
11. Snigirev O V et al. *Phys. Rev. B* **55** 14429 (1997)
12. Snigirev O V et al. *Fiz. Tverd. Tela* **40** 1681 (1998) [*Phys. Solid State* **40** 1530 (1998)]
13. Gudoshnikov S A et al. *Appl. Supercond.* **5** (7–12) 313 (1998)